RSC Advances

A Novel Potentiometric Self-plasticizing Polypyrrole Sensor Based on Bidentate bis-NHC Ligand for Determination of Hg (II) Cation

Journal:	*RSC Advances*
Manuscript ID:	RA-ART-06-2015-010950.R2
Article Type:	Paper
Date Submitted by the Author:	19-Aug-2015
Complete List of Authors:	Said, Nur Rahimah; University Malaya, Chemistry Rezayi, Majid; University of Malaya , chemistry Narimani, Leila; University Malaya, Chemistry Abdul Manan, Ninie; University Malaya, Chemistry Alias, Yatimah; University Malaya, Chemistry

A Novel Potentiometric Self-plasticizing Polypyrrole Sensor Based on Bidentate bis-NHC Ligand for Determination of Hg (II) Cation

Nur Rahimah Said[a,b], Majid Rezayi[a*], Leila Narimani[a], Ninie Suhana Abdul Manan[a], Yatimah Alias[a**]

[a]University of Malaya Centre for Ionic Liquid, Chemistry Department, Faculty of Science, University of Malaya, 50603 Kuala Lumpur, Malaysia.
[b]School of Chemistry and Environment, Faculty of Applied Science, Universiti Teknologi Mara Shah Alam, 40450 Shah Alam, Selangor, Malaysia.

Corresponding Authors: *chem_rezayi@yahoo.com
** yatimah70@um.edu.my

Abstract

In this approach, a new potentiometric self-plasticizing polypyrrole sensor was constructed based on a bidentate bis-NHC ligand for the purpose of Hg^{2+} cation determination. An ionophore, namely bis[1-benzyl-benzimidazoliumethyl]-4-methylbenzenesufonamide bromide (NHCL) was successfully synthesized and characterized using FT-IR, ^{1}H NMR, ^{13}C NMR spectroscopy, CHN elemental analysis, X-ray single crystal diffraction and UV-Vis spectroscopy. The electrode with a membrane optimum composition had demonstrated a good Nernstian response to Hg^{2+} cations ranging from 1.0×10^{-6} to 1.0×10^{-2} M with a detection limit of 2.5×10^{-7} M and a Nernstian slope of 28.10 ± 0.29 mV $decade^{-1}$ over a pH range between 4.5-7.0 with a response time of about 20 seconds at room temperature. The electrode exhibited better selectivity towards Hg^{2+} ions in comparison with some soft and hard metals; most of these metal ions do not show significant interference ($K^{pot}_{Hg^{2+},M}$). The proposed electrode also applies in the direct determination of Hg^{2+} cations in aqueous solution with sensible accuracy and precision.

Keywords: potentiometric; self-plasticizing; polypyrrole membrane sensor; bidentate bis-NHC ligand; Hg^{2+} cation; Nernstian response.

1. Introduction

According to the Agency for Toxic Substance and Disease Registry (ATSDT), in 2011 mercury was ranked as one of the top three hazardous substances. This is due to its toxicity, mobility and its ability to remain longer in the atmosphere [1-3]. Mercury can be absorbed by humans and other

organisms and can lead to serious health problems such as Amyotrohic lateral sclerosis, Alzheimer's disease, and Parkinson's disease. This metal can also damage kidneys and the immune system [4-6]. Therefore, there is a strong need to develop new methods to determine mercury (II) ions in our surroundings.

The construction of Ion Selective Electrodes (ISE) based on polyvinyl chloride (PVC) membrane is widely applied to the determination of Hg^{2+} ions [7] in various industrial, environmental and biochemical samples. Nevertheless, it made many problems when used for fabrication of solid-state sensors due to its poor adhesion on solid substances by solvent casting procedures which is requiring a plasticizer as a toxic material for the purpose of softening the polymer [8, 9]. The addition of plasticizers to make PVC flexible causes it's leaking into the solution during measurements and makes it the main cause of toxicity, a particular environmental concern [10-14].

Thus, these problems can be resolved with the use of a photo-curable and self-plasticizing polymer technique. The idea of a self-plasticizing membrane for ISE was developed recently where the acrylic membrane material has been shown to yield functional ion sensors without the incorporation of plasticizers [9].

Moreover, the use of conducting polymers in the structure of polymeric membrane sensor based on conductometric and voltametric methods have been reported recently[15-19]. Oxidized conducting polymers such as polypyrrole (PPy), polyaniline (PANI) and polythiophene (PT) having charge-compensating ions and poly cationic backbones can have effects on the potentiometric responses as ionic exchangers [20]. Among the reported conducting polymes, PPy was choosed in this study because of its wide range of uses, its simple mechanism for polymerization and its perm-selectivity for different ions. As reported previously, by adding specific ion-recognition sites on the conducting polymer membranes, the nonselective response of PPy towards specific cations can be extremely enhanced [21, 22].

The choice of ionophore as a recognition element is a very important factor that determines the selectivity of a particular ion among the other ions present in the solution[23-25]. Therefore, the synthesis of novel molecular ionophores to selectively recognized ionic species have engrossed increasing interest due to its important role and applications in clinical analyses[26, 27], environmental control [28, 29] and industrial processes. In the fabrication of ion selective electrodes (ISEs), various types of organic[30-33] and inorganic compounds such as acrylic compounds [34], crown ethers [35] and phosphenes [36] have been tested to be used as sensing elements.

To our own knowledge, there have been no reports of the use of bidentate bis N-Heterocyclic ligand (NHCL) as an ionophore in ISE applications. Thus, this reason encourages us to develop an ISE for the detection of mercury (II) cations based on NHCL as an ionophore. NHCLs are synthesized from benzimidazole and are found to be attractive ligands for complexation with metal cations due to their structure variety and stability [37]. The bind between mercury (II) cations and NHCL via the C carbene (-N*C*N-) atom is established via the coordination chemistry of organomercury (II) [38, 39]. NHCL was found to be a better donor than the best phosphine donor ligand and behave like a typical σ-donor ligand via substitution of classical $2e^-$ donor ligands such as phosphine, amines and ethers in metal coordination chemistry [40, 41]. Due to such ability, NHCLs emerge as a new class of versatile ancillary ligands in organic chemistry and often used as a valid alternative to the wide use of phosphine ligands. The application of NHCL as phosphine mimicking the ISE area as an ionophore can be explored.

In this study, a mercury (II)-cation selective electrode is fabricated using a photocurable pyrrole, including the new reported synthesized NHCL as an ionophore. The PPy membrane is formed on a 2-hydroxyethyl methacrylate (HEMA) initial layer that is polymerized on the surface of a screen printed electrode by a photocuring self-plasticizing method. For the best of our knowledge, there aren't any reports for fabrication of ISEs via the self-plasticizing method using a PPy and the obtained results presented herein will lay a strong foundation for the future design of PPy films, including the ionophores in the fabrication of ISEs.

2. Experimental

2.1 Reagents and Instrumentation

Chemicals and solvents such as benzylbromide, mercury acetate (Merck, Germany), 1,4-dioxane, diethy ether and acetonitrile (Fisher, United Kingdom) were used in synthesis part. In the sensor study, chemicals such as 2,2-dimethoxy-2-phenylacetophenone (DMPP), pyrrole, , 2-hydroxyethyl methacrylate (HEMA), ethylenediaminetetraacetic acid (EDTA), sodium tetraphenylborate (NaTFB), hydrochloric acid (HCl), and sodium hydroxide (NaOH) were purchased from Sigma-Aldrich (USA) and Merck (Germany). All the metal ions used were chloride salts purchased from Sigma-Aldrich (USA), Fisher (United Kingdom) and Merck

(Germany). The stock solution (10^{-1}M) was prepared by dissolving $HgCl_2$ (Merck, Germany) in DI-water. Other diluted solutions were prepared from this stock solution. All chemicals were of analytical grade and used without further purification.

The difference in cell potential or electromotive force (emf) in mV of ISE potentiometric sensors was measured in connection with a Ag-AgCl double-junction reference electrode (Thermo Orion 900200) using a digital pH/ISE meter (Orion Star A214). The electrochemical impedance spectroscopy (EIS) was performed using a potentiostat/galvanostat (PGSTAT-302N, Autolab), controlled by a USB IF030 interface (Metrohm Autolab). All measurements were carried out at room temperature. The melting points of samples were measured using a U Met-temp II Laboratory Devices USA. The FTIR spectra were recorded between 4000-400 cm^{-1} as attenuated by the total reflectance (ATR) on Perkin Elmer Spectrum 400 FTIR spectrometer. ^{1}H and ^{13}C Nuclear Magnetic Resonance (NMR) were recorded on a Bruker Advance 400 spectrometer at 400 MHz using tetramethylsilane (TMS) as the internal standard. The CHN elemental analysis value for NHCL was determined using a Perkin Elmer CHNS/O 2400 Series II. The crystal data was collected from a Bruker SMART APEX2 diffractometer and the structure of NHCL was solved using direct methods and refined by full-matrix least squares using the program SHELXTL-97 Sheldrick. The spectrophotometer type UV/Vis/NIR (UV- 3600 Shimadzu) including the temperature controller TCC-2 was used to obtain the spectra of NHCL inophore, Hg^{2+} cation and resulted complex respectively. Morphology of membranes was analyzed using a Field Emission Scanning Electron Microscope HITACHI SU8220 equipped with Energy Dispersive facility (FESEM-EDX). The structure crystallinity of membrane was examined using powder X-Ray Diffraction (XRD) PANalytical EMPYREAN at room temperature and scanned from 20º to 80º 2θ angles using a step interval of 0.02º and scan speed of 5º min^{-1}.

2.2 Preparations

2.2.1 *Synthesis and characterization of NHCL*

For synthesis of NHCL, N,N-bis[(Benzimidazol-1-yl)ethyl]-4-methylbenzenesulfonamide (0.2296 g, 0.5 mmol), benzylbromide (0.1710 g, 1.0 mmol) and 20 mL 1,4-dioxane were placed in a 100 mL round bottom flask. The reaction mixture was stirred and refluxed at 100 ºC for 12 hours and a pale yellow precipitate was obtained. The product was collected using filtration,

washed with fresh 1,4-dioxane (2×5 mL) and diethyl ether (2×5 mL) and dried in vacuo to obtain pale yellow powder. The N,N-bis[(Benzimidazol-1-yl)ethyl]-4-methylbenzenesulfonamide was prepared according to the method reported previously[42]. (Yield: 98%, m.p: 393K). Spectroscopic analysis: IR (cm^{-1}): 3124, 3020 $(C\text{-}H)_{Ar}$, 2810 $(C\text{-}H)_{Aliph}$, 1565 (C=N), 1494, 1452 $(C{=}C)_{Ar}$, 1341,1163 (O=S=O); ^{1}H-NMR (DMSO-d_6) δ ppm: 10.24 (s, 2H, $C\text{-}H_{Carbene}$), 8.16 (d, J=8Hz, 2H, $C\text{-}H_{Ar}$), 8.00 (d, J=8Hz, 2H, $C\text{-}H_{BIm}$), 7.73 (m, 4H, $C\text{-}H_{BIm}$), 7.62 (d, J=8Hz, 4H, $C\text{-}H_{Ar}$), 7.44 (m, 8H, $C\text{-}H_{Ar}$), 7.15 (d, J=8Hz, 2H, $C\text{-}H_{BIm}$), 5.90 (s, 4H, $Ph\text{-}CH_2$), 4.94 (t, J=8Hz, 4H, $CH_2\text{-}N_{BIm}$), 4.02 (t, J=8Hz, 4H, CH_2-N), 2.34 (s, 3H, $-CH_3$); ^{13}C-NMR (DMSO-d_6) δ ppm: 144.28 (1C, $C_{Ar\text{-}S}$), 143.22 (2C, $C_{Carbene}$), 135.21 (1C, $C\text{-}CH_3$), 134.33 (2C, C_{BIm}), 131.79 (2C, C_{BIm}), 131.16 (2C, $C_{Ar}\text{-}CH_2$), 130.09 (2C,CH_{BIm}), 129.40 (2C, CH_{Ar}), 129.20 (4C, CH_{Ar}), 128.78 (4C, CH_{Ar}), 127.28 (2C, CH_{Ar}), 126.98 (4C, CH_{BIm}), 114.35 (2C, CH_{BIm}) , 114.18 (2C, CH_{Ar}), 50.36 (2C, $Ph\text{-}CH_2$), 46.73 (2C, CH_2-N), 45.44 (2C, $CH_2\text{-}N_{BIm}$), 21.48 (1C, CH_3). Elemental analysis; calculated: C, 58.43; H, 4.90; N, 8.74; found: C, 57.40; H, 5.14; N, 8.54.

The molecular structure of NHCL was demonstrated using a single X-ray analysis. The crystallinity of the targeted compound, suitable for X-ray diffraction was obtained using slow evaporation of a solvent mixture of MeOH / H_2O at room temperature. The NHCL crystallized as a triclinic lattice containing a pair of bromide anions in asymmetric unit with space group of $P\bar{1}$, a = 14.7495(9) Å, b = 15.5216(8) Å, c = 19.1751(10) Å, α =108.720(5), β = 100.073(5), γ= 108.177(5), V = 3761.1(3) $Å^3$, T = 100 (2) K and Z = 2 as the refinement data are shown in Table 1. Figure 1 shows the numbering scheme of molecular structure.

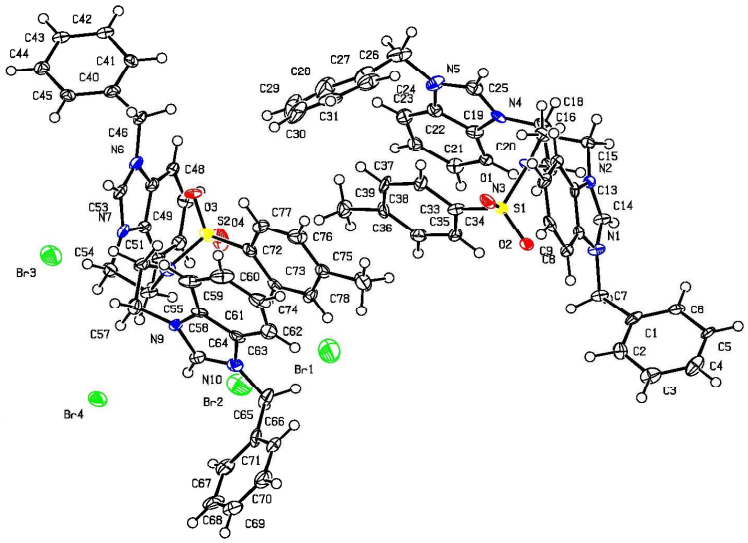

Figure1: ORTEP diagram of a symmetric unit of NHCL with thermal ellipsoids drawn at 50%

Probability

Table 1: Crystal data and structure refinement for Bis[1-benzyl-benzimidazoliumethyl]-4-methylbenzenesufonamide bromide (NHCL).

Empirical formula	$C_{39}H_{39}Br_2N_5O_2S$
Formula weight	801.62
Temperature (K)	100.2(8)
Crystal system, Space group	Triclinic, P $\bar{1}$
a(Å), α(°)	14.7495(9), 108.720(5)
b(Å), β(°)	15.5216(8), 100.073(5)
c(Å), γ(°)	19.1751(10), 108.177(5)
Volume ($Å^3$)	3761.1(4)
Z, Calculated density (g/cm^3)	2, 1.416
μ/mm^{-1}	2.251
F(000)	1640.0
Crystal size (mm^3)	0.22 × 0.15 × 0.12
Radiation	Mo Kα (λ = 0.71073)
Theta range for data collection	2.929-26.50
Index ranges	$-20 \leq h \leq 20$, $-22 \leq k \leq 20$, $-26 \leq l \leq 25$
Reflections collected	44481
Independent reflections	15582 [R_{int} = 0.0849, R_{sigma} = 0.1749]
Data/restraints/parameters	15582/ 0/ 849
Goodness-of-fit on F^2	1.072
Final R indexes [I>=2σ (I)]	R_1 = 0.0977, wR_2 = 0.2737
Final R indexes [all data]	R_1 = 0.1610, wR_2 = 0.3140
Largest diff. peak/hole / e $Å^{-3}$	2.22/-2.81
CCDC Number	1051318

Table 2: Selected bond length (Å) and bond angles (°)

Atoms	Angles	Atoms	Angles
N1 - C14	1.323(11)	O1 - S1 - O2	118.7(4)
N2 - C14	1.336(9)	O1 - S1 - N3	106.4(4)
N5 - C25	1.343(11)	N4 - C25 - N5	112.1(8)
N4 - C25	1.312(11)	C24 - N5 - C26	126.2(7)
N5 - C26	1.509(11)	O1 - S1 - C33	110.0(4)
N1 - C7	1.479(10)	N5 - C24 - C23	132.0(7)
C1 - C7	1.535(10)	N5 - C26 - C27	113.6(8)
C26 - C27	1.452(16)	N5 - C24 - C19	106.6(7)
S1 - N3	1.649(7)	N1 - C14 - N2	110.9(7)
S1 - O1	1.432(7)	C7 - N1 - C8	126.6(7)
S1 - O2	1.433(6)	C7 - N1 - C14	124.4(7)

Table 3: Selected hydrogen bond geometry (Å, °) for crystal.

D—H…A	D—H	H…A	D…A	D—H…A
C9-H9…O1^{i}	0.95	2.45	3.285(10)	147
C15-H15A…Br1^{ii}	0.99	2.87	3.763(8)	151
C16-H16A…O1	0.99	2.36	2.825(11)	108
C26-H26A…Br3^{iii}	0.99	2.81	3.712(10)	152
C26-H26B…Br3^{ii}	0.99	2.92	3.880(10)	163
C34-H34…O2	0.95	2.52	2.884(10)	103
C48-H48…O4^{iv}	0.95	2.44	3.178(12)	134
C53-H53…Br4^{v}	0.95	2.83	3.324(8)	114
C55-H55B…O4	0.99	2.34	2.790(12)	106
C56-H56B…O3	0.99	2.58	2.933(11)	101
C57-H57A…Br3	0.99	2.79	3.675(9)	149
C57-H57B…Br4	0.99	2.71	3.646(9)	159
C65-H65B…Br2	0.99	2.88	3.775(10)	150
C77-H77…O3	0.95	2.47	2.859(10)	105

Symmetry codes: (i) 1-x,-y, 2-z, (ii) -1+x, y, z (iii) 1-x,-y, 1-z, (iv) 1-x, 1-y,1-z, (v) 2-x, 1-y,1-z

There are two molecules per asymmetric unit cell. The whole molecule is not planar and the benzimidazolium dication is centrosymmetric. Table 2 complies selected bond lengths and angles which are all in normal ranges. The N1-C14, N2-C14, N4-C25 and N5-C25 bond lengths are similar (1.30 Å) indicating a delocalization of electron about the N—C—N bond. The structure is stabilized by C-H..O and C-H..Br inter and intra molecular hydrogen bonds (symmetry codes: (i) 1-x,-y, 2-z, (ii) -1+x, y, z (iii) 1-x,-y, 1-z, (iv) 1-x, 1-y,1-z, (v) 2-x, 1-y,1-z),

forming a three-dimensional network (Figure 2). All the hydrogen bondings and geometries are summarized in Table 3. The crystallographic data of NHCL crystal was deposited with the Cambridge Crystallographic Data Centre (CCDC) reference Number of 1051318[43-45].

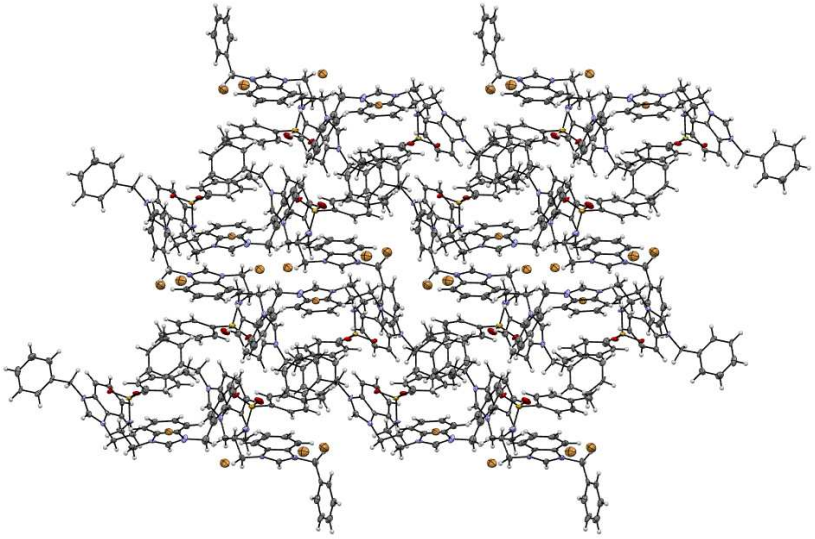

Figure 2: Molecular packing of NHCL viewed down b-axis.

The NHCL-Hg^{2+} complex was prepared by adding 0.16 g $Hg(OAc)_2$ to a suspension of 0.35 g NHCL in 40 mL acetonitrile. The solution mixture was refluxed for 24h and the formed complexes were filtered and washed with distilled water to obtain a white powder compound. The spectroscopic data shows an absence of peaks at 1560-1570 cm^{-1} in FTIR spectra, an absence of chemical shift signals at δ 10.00 ppm in ^{1}H-NMR spectra and the changes of chemical shift signal positions to the lower fields at δ 185.97 in ^{13}C-NMR spectra in comparison to the NHCL spectra which prove that the complexation of NHCL with mercury occurred at $C_{carbene}$ position [46, 47]. Figure 3 shows the optimized structure of NHCL ionophore and NHCL-Hg^{2+} complex obtained from the GAUSSIAN 09 program based on the density functional theory (DFT/B3LYP).

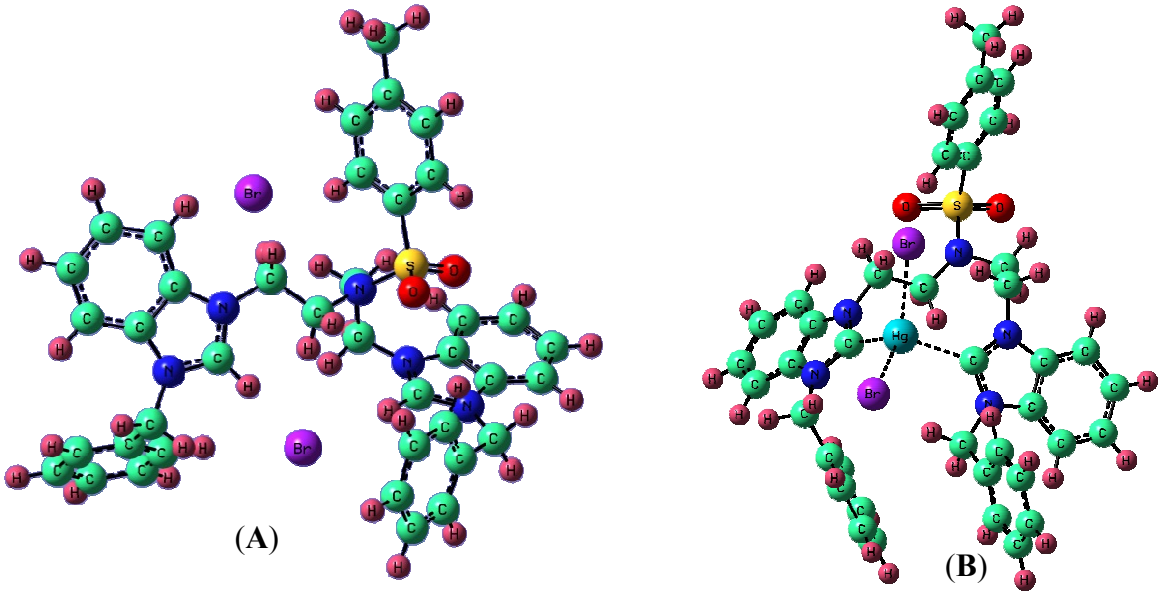

Figure 3 : Optimized structure of (**A**) NHCL ionophore and (**B**) NHCL-Hg^{2+} complex

Complexation reaction between NHCL ligand and Hg^{2+}cations leads to synthesis of Hg-carbene complex. In this reaction, the $HgCl_2$ metalic salt precursor is acting as a base for deprotonation of the imidazolium salt, leading to the coordination of Hg^{2+} metal cations to the intermediate carbene of NHCL and the counter-anions (Br^-) attached to the ligand [2, 48]. The schematic of complex reaction is expressed as follow:

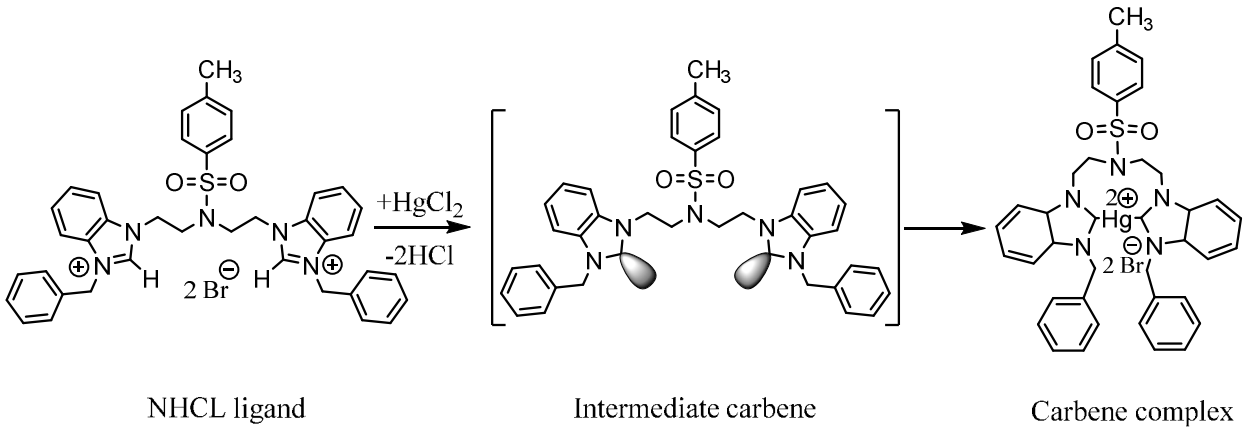

Schematic 1: Complex reaction mechanism of NHCL with Hg^{2+} cation

The preliminary spectrophotometrically study of the complexation of NHCL ionophore with Hg^{2+} cation was carried out based on three solutions, NHCL inophore in 1.00×10^{-4}M, $HgCl_2$ with a concentration of 1×10^{-4}M and their 1:1 mixtures in pure DMSO solvent. The spectra were recorded from 250 to 300 nm. As obvious in Figure 4, the spectrum of $HgCl_2$ shows two absorption maxima at 253 and 262 nm while the NHCL ionophore spectrum shows two absorption maxima at 268 and 272 nm. With the addition of $HgCl_2$ to the NHCL ionophore, the blue absorption band slightly shifted and its intensity increased. The observed behavior proves the special tendency of NHCL ionophore towards Hg^{2+} cations and confirms its selective interaction.

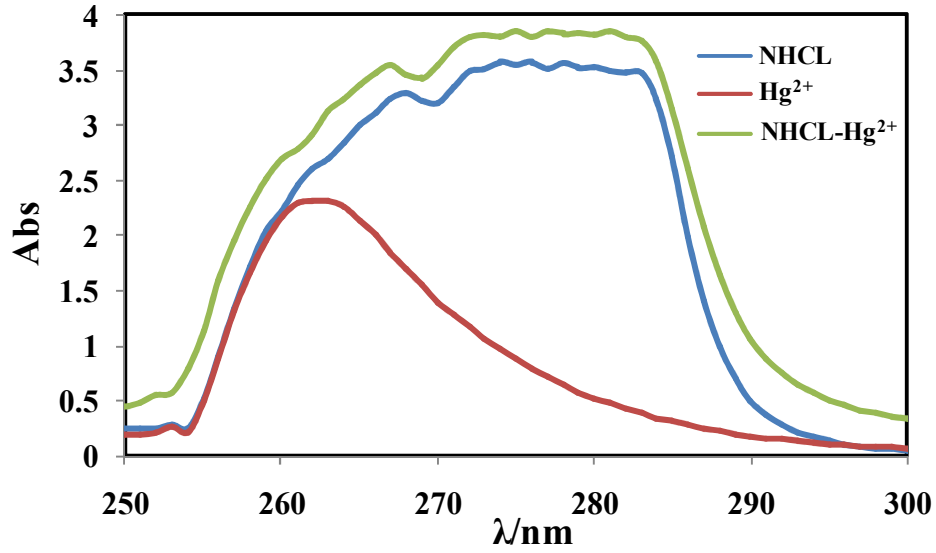

Figure 4: UV-Vis absorption spectra of 1.0×10^{-4}M $HgCl_2$, 1.0×10^{-4}M NHCL ionophore and 1:1 (V/V) mixture of NHCL ionophore and $HgCl_2$ solution.

2.2.2 Sensor fabrication

The sensor membranes were fabricated and photocured according to the modification method reported previously [34]. The procedure to prepare ISE membrane was as follows: First, a layer containing a mixture of 96.8wt% HEMA (monomer) and 3.2 wt% DMPP (photoiniator) was deposited on the tip of a silver/silver chloride screen printed electrode (SPE). 0.2 µL of the mixture was photocured under UV radiation (15w Blacklight F15T8/BL 15 watt; Peak Emission

365 nm) with a constant flow of nitrogen gas for 480s. Second, the obtained membrane is then destocked in 0.01 M of mercury (II) chloride solution for 20 min to form the "inner solution" of the sensor. Finally, 0.5 μL of the mixture with various compositions as mentioned in Table 4 (pyrrole (monomer); DMPP (photoiniator); NaTFB (additive) and NHCL (ionophore)) was then deposited on top of the hydrated poly-(HEMA) inner layer using the photocuring technique as before.

2.2.3 Sensor evaluation

The responses of the sensors were measured in an electrochemical cell setup. A double-junction Ag/AgCl was used as an external reference electrode with a reference solution (3M KCl) as the inner filling solution (Orion 900002) and 0.1 M lithium acetate (LiOAc) as a gel bridge electrolyte. The Hg^{2+} ISE membrane was prepared according to the mentioned method and used as a working electrode. Both electrodes were connected to an Orion pH/ISE-meter. All testing solutions of mercury (II) chloride were prepared in the deionized water in concentrations ranging from 1×10^{-8} to 1×10^{-1} M. The potential readings for the mercury solution starting from the low to high concentrations were recorded when a stable value (mV) was reached after 20 seconds. The call potentials were measured using a schematic galvanic cell as follows:

Ag | AgCl(s) | KCl (3 M) | bridge electrolyte | test solution | NHCL-PPy membrane | inner filling membrane layer | AgCl(s) | Ag

3. Results and discussion

3.1. Influence of the electrode composition and calibration curve

The composition of plasticizer-free membranes with covalently bound ion-recognition sites can affect the potentiometric response and detection limit of sensors. Several studies on the membrane composition of electrodes have reported significant influence on the selectivity and sensitivity of produced ion selective electrodes [1-3]. Thus in this studies the electrode membrane was optimized by varying the ratio of its compositions as shown in Table 4. From the results, the electrode without ionophore showed a slightly weak potentiometric response towards Hg^{2+} cation (E5). This is why the NHCL ionophore plays the most important role in the proposed ISE

membrane composition for the sensing of Hg^{2+} cations. The observed potentiometric response can be related to the properties of NHCL ionophore as the active component of potentiometric sensors toward the target ions and the presence of lipophilic salt, NaTFB in the membrane. The use of PPy as the membrane matrix leads to produce the plasticizer-free bulk membrane. The optimum membrane composition was obtained using 89.4 wt.% monomer pyrrole, 4.8 wt.% photoinitiator DMPP, 0.2 wt.% lipophilic salt NaTFB, and 5.6 wt.% ionophore NHCL (E3). The electrode without NaTFB additive exhibited the non-Nernstian potential response slope (E6). The ion-pairing can be kept low by incorporating an inert lipophilic salt or the largest of anionic site additives, sodium tetrakis(4-chlorophenyl)borate. It is well known that the addition of lipophilic salts in membrane composition diminishes its ohmic resistance and enhances its responsive behavior [49]. This is demonstrated by the data in Table 4 that the presence of NaTFB in the membrane composition is needed in order to reduce resistance and maintain conductivity to optimize the selectivity and sensitivity of the membrane sensor. By increasing the lipophilic anion, NaTFB showed deviation from the Nernstian response of the proposed electrode (E1). Several reasons for such behaviors (super-Nernstian slopes) have been reported for conventional polymeric sensors based on non-plasticized membranes [50, 51]. Among them, the nature of the conducting substrate, specially the nature of NHCL ionophore/NaTFB additive ratio, pH interferences and the dielectric constant of membrane were mentioned as the most effective parameters. The excessive influx of primary ions from the sample phase into the inner electrolyte and a resultant depletion of sample ions in the diffusion layer at the sample-membrane phase boundary was another effective factor showing this behavior[52, 53]. The enhancement amount of ionophores as the sensing element of membrane composition in Table 4 verified this fact using covalent bonding with Hg^{2+} cations in the membrane (E9 & E10).

The comparison of the calibration plot of mercury (II) ion selective electrodes with and without ionophores and without additive is presented in Figure 5. Electrode E3 gave the best response based on its Nernstian slope, working range as well as detection limit as compared to electrodes E5 and E6. It exhibited a Nernstian slope of 28.16 mV per decade in a wide concentration range between 1×10^{-6} and 1×10^{-2} M. The detection limits for electrodes were determined according to the cross-section of two extrapolated calibration graphs to the baseline potential of 2.5×10^{-7} M [54].

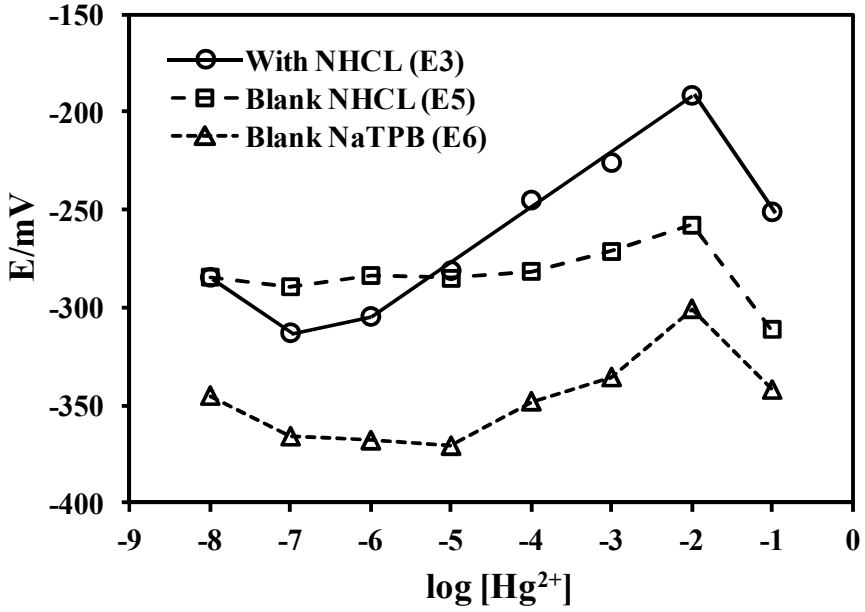

Figure 5: Calibration plot of the optimized mercury ion-selective sensor

Table 4: The composition of ISE membrane used based on NHCL ionophore for the potentiometric detection of Hg^{2+} cation

electrode	Composition (w/w %)				Electrode characteristics			
	pyrrole	DMPP	NaTFB	NHCL	Slope (mV/decade)	LR (M)	LOD (M)	R^2
E1	91.8	2.4	0.8	5.0	38.99	1×10^{-6}-1×10^{-1}	2.0×10^{-7}	0.98
E2	89.4	4.8	0.8	5.0	37.03	1×10^{-5}-1×10^{-1}	2.5×10^{-6}	0.95
E3*	89.4	4.8	0.2	5.6	28.16	1×10^{-6}-1×10^{-2}	2.5×10^{-7}	0.99
E4	94.2	0	0.2	5.6	26.30	1×10^{-5}-1×10^{-3}	6.3×10^{-6}	0.98
E5	95.0	4.8	0.2	0	11.80	1×10^{-4}-1×10^{-2}	7.9×10^{-5}	0.99
E6	89.6	4.8	0	5.6	22.27	1×10^{-5}-1×10^{-2}	1.6×10^{-6}	0.97
E7	91.0	4.8	0.2	4.0	23.97	1×10^{-5}-1×10^{-2}	3.2×10^{-6}	0.98
E8	89.5	4.8	0.1	5.6	26.58	1×10^{-5}-1×10^{-2}	4.0×10^{-6}	0.98
E9	89.0	4.8	0.1	6.1	36.92	1×10^{-5}-1×10^{-2}	4.0×10^{-6}	0.99
E10	88.2	5.2	0.1	6.5	39.12	1×10^{-4}-1×10^{-2}	8.9×10^{-5}	0.98

*Optimum membrane composition.

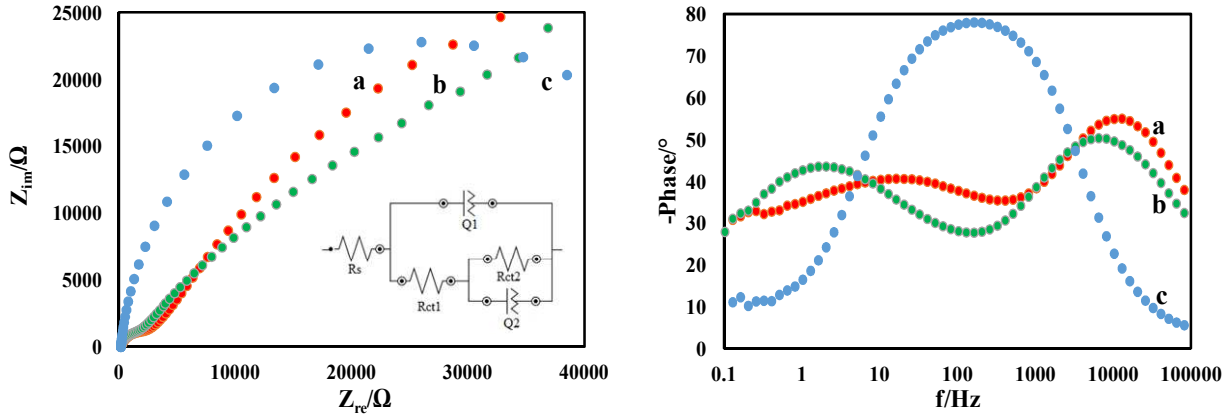

Figure 6: Nyquist and phase plots of the impedance spectra recorded for optimized membranes (a) without, (b) with NaTFB additive and (c) without NHCLionophore.

Table 5: Impedance parameters for electrodes E3, E6 and E5 (Table 4) as determinate using the equivalent circuit presented in Figure 6.

electrode	R_s *(Ω)*	R_{ct1} *(KΩ)*	Q_1 (nMho)	n_1	R_{ct2} *(KΩ)*	Q_2 (µMho)	n_2
E3	97.9	1.57	182	0.82	153	13.7	0.48
E6	101	2.97	646	0.74	111	12.3	0.62
E5	113	50	772	0.91	-	-	-

The electrochemical impedance spectroscopy (EIS) was performed in 1 mM $Fe[(CN)_6]^{3-/4-}$ (1:1) containing 0.1 M KCl solution to investigate the role of NaTFB additive for improving the potential response of the proposed membrane sensor by reducing the ohmic resistance of polymeric membrane[55, 56]. EIS data were recorded at open circuit potential with an AC amplitude of 5 mV and a frequency range from 100 kHz to 0.1 Hz by using the potentiostat/galvanostat with a platinum and SCE as counter and reference electrodes, respectively. The impedance spectra for optimized membrane recorded with and without NaTFB additive showed two charge-transfers which were fitted to the equivalent circuit presented at Figure 6 and fitting results are summarized in Table 5. First charge-transfer is related to the outer layer (PPy layer), while the second charge-transfer is related to the inner layer (HEMA layer). From Figure 6 and from fitting results summarized in Table 5, it is obvious that presence of NaTFB additive causes to reduce $R_{ct.}$ Moreover, the absence of NHCL ionophore in the membrane composition leads to enhance the charge transfer resistance, and also a tight structure of PPy membrane which is showed only

a charge-transfer PPy outer layer connected to the electrolyte. This is because of the presence of ionophore increases electrical conductivity and hence the charge transfer resistance decreases. The comparison of the semicircle diameters from the Nyquist plots of the modified electrodes presents the following direction of R_{ct} (Table 5): *(R_{ct1}): E3> E6>E5.*

3.2 Potential response for various cations:

To compare the selectivity of membrane electrode based on the NHCL ionophore toward the Hg^{2+} cation over other cations, the optimized membrane sensor was used over a wide concentration range of 1.0×10^{-8}M to 1.0×10^{-1}M of various cations and the results showed in Figure 7. As can be seen from the all tested cations, Hg^{2+} cation exhibited the best Nernstian response with the slope of 28.16 mV per decade and seemed to be suitably determined by the membrane sensor based on NHCL ionophore. It can be justified due to the strong selective complexation behavior of the ionophore towards Hg^{2+} compared to other metal ions as well as the rapid exchange kinetics of the obtained complex. Therefore, NHCL was used as a suitable ionophore in the fabrication of Hg^{2+}-ISE.

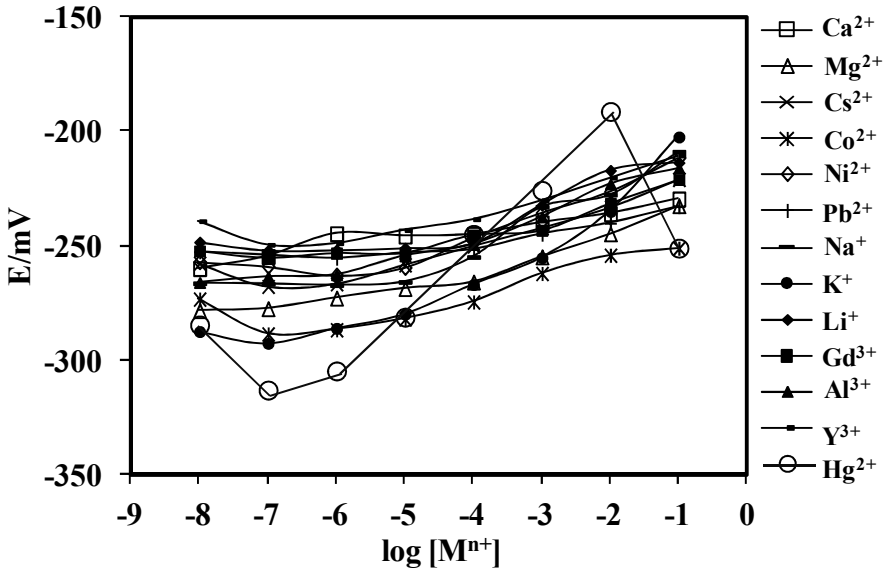

Figure 7: Potential response of optimized membrane electrode (electrode no. E3) based on NHCL ionophore for various metal cations.

3.3 Effect of pH on electrode performance

The pH effects of the test solution on potential response were studied at fixed concentrations and temperatures. The potential values of the test solution in concentrations of 1×10^{-5} and 1×10^{-3}M were recorded over the pH range of 1.0-8.0, respectively. HCl and NaOH solutions were used to adjust the pH of the test solutions at the required values. The results in Figure 8 revealed that the electrode response was pH independent in the range of 4.5-7.0. However it showed a reduce in potential values at pH range lower than 4.5 and higher than 7.0. This is evidence that under more acidic environments, partial protonation of ion carrier happens, causing the loss of tendency to build complex structures with metal cations [50, 57]. While in a basic environment, the potential decrease is attributed to the formation of $Hg(OH)^+$ in the test solution according to the chemical equilibrium: $Hg^{2+}+OH^-\rightarrow Hg(OH)^+$ which is coordinated with the ionophore in the membrane. The formation of Br_2NHCL^--$Hg(OH)^+$ ion-pairs in the membrane leads to the increase of $Hg(OH)^+$ extraction in the $HgCl_2$ solution and its complexation into the membrane sites can be another factor in the potential response of Hg(II) selective electrodes at higher pH [58, 59].

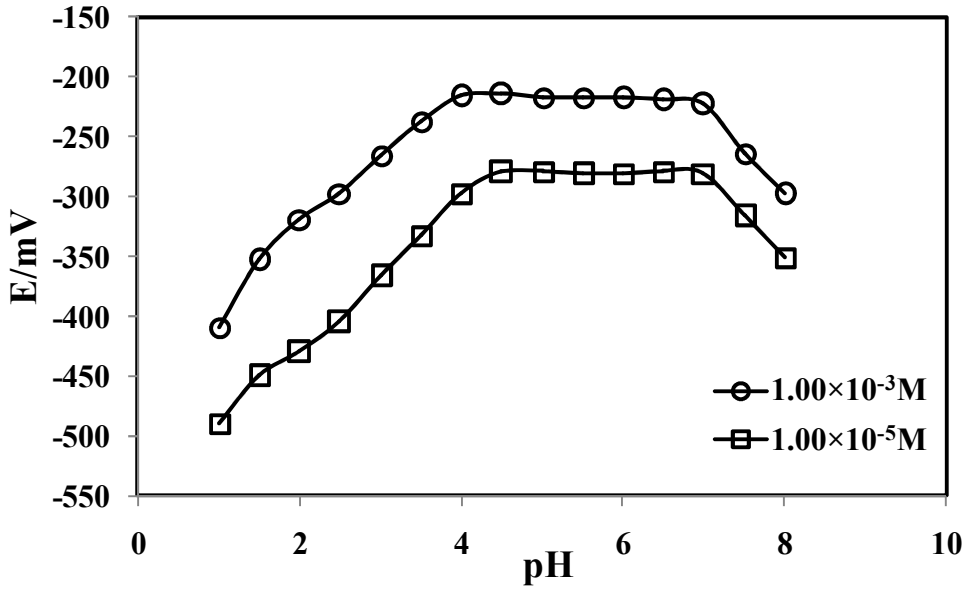

Figure 8: Effect of pH test solutions on the response of the proposed Hg(II)-ISE in different concentrations.

3.4 Determination of selectivity coefficients

The potentiometric selectivity coefficients $\left(K_{Hg^{2+},M}^{pot}\right)$ were evaluated using the separation solution (SSM) and matched potential (MPM) methods according to IUPAC recommendations [60]. In SSM, the difference of potential between the reference electrode and membrane electrode is measured according to the two separate solutions of Hg^{2+} and M, where M is the interfering cation at the same activity ($a_{Hg^{2+}} = a_{M^{n+}}$). Selectivity coefficients used the following equation:

$$K_{Hg^{2+},M^{n+}}^{SSM} = a^{(1-2-n)} e^{(E_M - E_{Hg^{2+}})2F/(RT)} \quad (1)$$

Where $K_{Hg^{2+},M^{n+}}^{SSM}$ is the potentiometric selectivity coefficient, $E_{Hg^{2+}}$ is the potential measured in 1×10^{-3}M of the Hg^{2+} cation solution, E_M is the potential measured in 1×10^{-3}M of the interfering cations (M), F is the Faraday constant, R is the gas constant at room temperature and n is the charges of interfering cations.

Meanwhile in MPM, the selectivity coefficient of proposed sensors is calculated based on the ratio of primary and interfering ions under the same conditions that give the identical potential changes. In this study, the known activity (1×10^{-1} M) of the primary ion, $a'_{Hg^{2+}}$ solution is added into a reference solution that contains a fixed activity (1×10^{-3} M) of primary ions, $a_{Hg^{2+}}$ and the changes of corresponding potential ($\Delta E_{Hg^{2+}}$) are recorded. After that, the interfering cation solution, $a_{M^{n+}}$ is added to the primary solution (reference solution) to reach the same potential change (ΔE_M). The potential change must be the same for both primary and interference ion as it is produced in a constant initial background of primary ions. Then, the selectivity coefficient resulted based on the following equation:

$$K^{MPM}_{Hg^{2+},M^{n+}} = (a'_{Hg^{2+}} - a_{Hg^{2+}}) / a_{M^{n+}} \quad (2)$$

All results from SSM and MPM methods are summarized in Table 7. It is obvious that the selectivity coefficients of electrodes toward interfering cations are lower than Hg^{2+} cations and most of the selectivity coefficients are very low, indicating no significant interference in the performance of the fabricated electrode for determining Hg (II) cations, except for lead (II) cations. It caused only a slight interference due to the existence of soft donor atoms (carbene) in the ionophore structure where Pb^{2+} and Hg^{2+} act as atypical intermediates and the soft acidic ions are more likely to build complex structures with the NHCL. However, Pb^{2+} does not cause any interference at low concentrations. All values are less than 1, showing that the ISE is more responsive to primary cations, which is Hg^{2+}. The $K^{pot}_{Hg^{2+},M}$ values obtained based on the two methods employed are similar.

Table 7: Selectivity coefficient values, K^{SSM} and K^{MPM} of various cations for the proposed Hg^{2+} ion selective electrodes

Interfering ion	($K^{SSM}_{Hg^{2+},M}$)	($K^{MPM}_{Hg^{2+},M}$)
Ca^{2+}	1.87×10^{-2}	1.37×10^{-2}
Mg^{2+}	8.94×10^{-2}	1.46×10^{-2}
Co^{2+}	7.25×10^{-2}	2.89×10^{-2}
Ni^{2+}	1.99×10^{-2}	7.04×10^{-2}
Pb^{2+}	1.23×10^{-1}	2.39×10^{-1}

Cs^{+}	1.88×10^{-2}	5.38×10^{-2}
Na^{+}	4.40×10^{-2}	1.45×10^{-2}
K^{+}	2.40×10^{-2}	2.61×10^{-2}
Li^{+}	9.32×10^{-1}	1.50×10^{-2}
Gd^{3+}	7.63×10^{-4}	1.36×10^{-3}
Al^{3+}	1.83×10^{-3}	1.03×10^{-2}
Yb^{3+}	5.99×10^{-4}	2.39×10^{-3}

3.5 Response time and life time

The response time of a sensor is considered as the required time of potential to reach a steady state within ±1mV during the immersion of sensor in a series of respective test solutions. In this study, the dynamic response time of proposed sensor was obtained by changing the concentration of solution from 1.0×10^{-6} to 1.0×10^{-2} M (low to high), sequentially. After successive immersions of proposed sensor into the solutions, the time needed to reach a potential within ±1mV of final equilibrium value was obtained at about 20 s, as clearly shown in Figure 9.

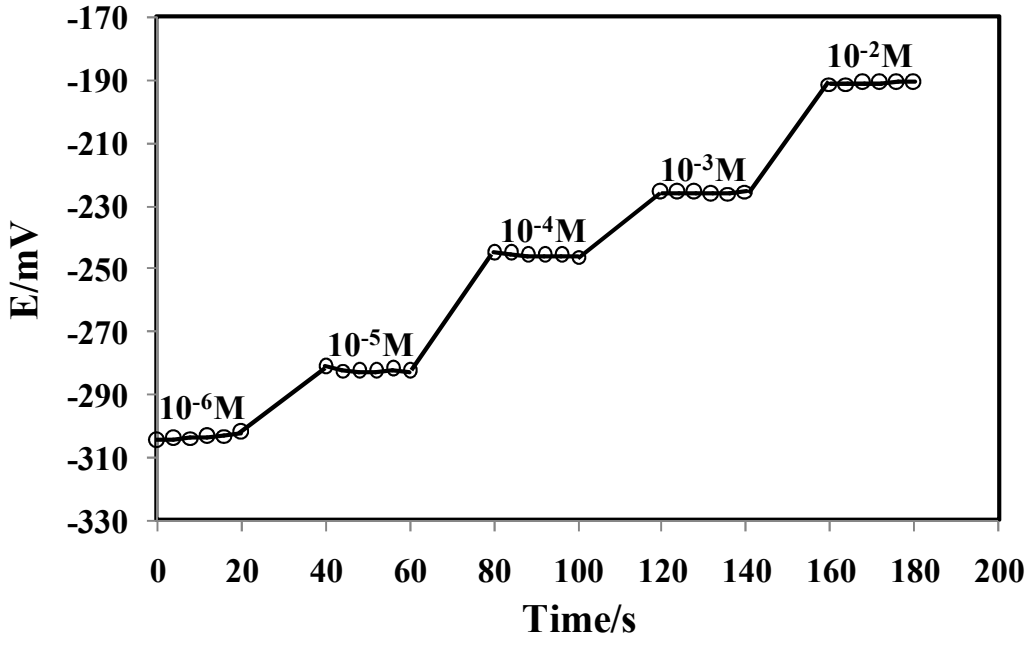

Figure 9: Dynamic response of the proposed electrode for the steps changes in Hg^{2+} concentration (from low to high).

The stability and lifetime of the proposed membrane sensor were evaluated using the proposed sensor at different time periods via 4 weeks, where there was no significant change in the Nernstian slope. During these times, the proposed sensor was used at least one hour per day. The limitation of lifetime in the fabricated proposed sensor could be due to the loss of membrane ingredients in the NHCL ionophore and its leaching into the sample solution.

3.6 Repeatability and reproducibility

To validate the proposed method, parameters such as repeatability and reproducibility of electrode were evaluated. The repeatability of the proposed sensor was tested using three measurements over the working concentration ranges of the optimized electrode membrane (E3) within a single day and the results are shown in Table 8. The average of slope obtained was 28.10 ± 0.26 mV decade^{-1} with a relative standard deviation (RSD) of 0.92%. This indicates high precision and accuracy of the proposed procedure.

The reproducibility of ISE was studied using three different optimum composition (E3) membrane electrodes, where each electrode was used only once. The results obtained are summarized in Table 6. Calculations made for all three electrodes gave the average and standard deviation of Nernstian slope and their values of 29.10 ± 0.82 mV per decade. The obtained values for relative standard deviation (RSD) were much lower than 5%, which can be considered as an acceptable value for repeatability and reproducibility studies. The variation of results in this study compared to the repeatability study could be due to the different thicknesses and morphology of the three different membranes at different locations, which resulted in fluctuations in the extraction equilibrium of corresponding ions at the vicinity of the interface between the membrane and aqueous layer, so the different Nernstian slopes from one electrode to another could be vindicated, consequently, the variation of thicknesses is proved to cause minor changes in the Nernstian slopes of the electrodes.

Table 8: The repeatability and reproducibility studies of optimize composition membrane electrode.

Study	Nernstian slope (mV decade^{-1})	Average	Standard deviation	*RSD*

Repeatability	28.16, 28.30, 27.80	28.10	0.26	0.92
Reproducibility	28.16, 29.53, 29.62	29.10	0.82	2.82

3.7 Characterization of membrane electrode

The proposed membrane sensor was examined using FTIR spectroscopy to observe the influence of ionophore in the PPy membrane. Figure 10 represents the characteristic peaks of FTIR spectra for (a) NHCL ionophore, (b) NHCL-Hg^{2+} complex, and (c) optimized PPy membrane after use. The FTIR spectra (a) show the complexation reaction between NHCL ligand and Hg (II) cation which leads to a significant band shift of (C=N) stretching peak from 1570 cm^{-1} in ionophore (a) to lower frequencies of about 1509 and 1421 cm^{-1} in complex (b and c) respectively due to the coordination of carbon to Hg^{2+} metal cation. On the other hand, the absence of C-H stretching band at above 3000 cm^{-1} is another proof for formation of complex from $C_{carbene}$ position. Spectrum (a) also show strong absorption peak at 550 cm^{-1} which is refer to the ionic bonding of C-Br in NHCL structure. However, after complexation with Hg^{2+}, the intensity of absorption peak at that position was reduced as shown in Figure 10.

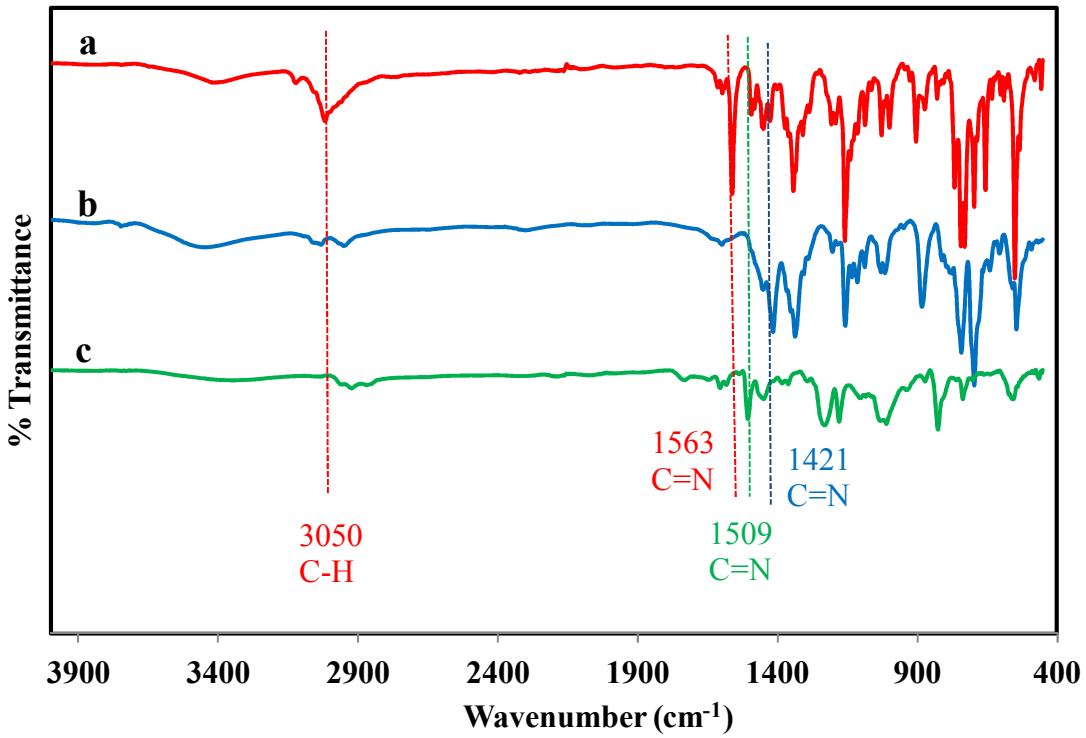

Figure 10: The FTIR spectra of the PPy membrane sensor based on NHCL ionophore: (**a**) NHCL ionophore, (**b**) NHCL-Hg^{2+} complex, and (**c**) fresh optimized PPy membrane after used.

Figure 11 shows the XRD pattern for optimized PPy membrane sensors after use. Results of analyses showed the presence of crystal phases and existence of mercury in optimized electrodes (E3) after the complexation with NHCL ionophores in the membrane (PDF≠00-023-1768).

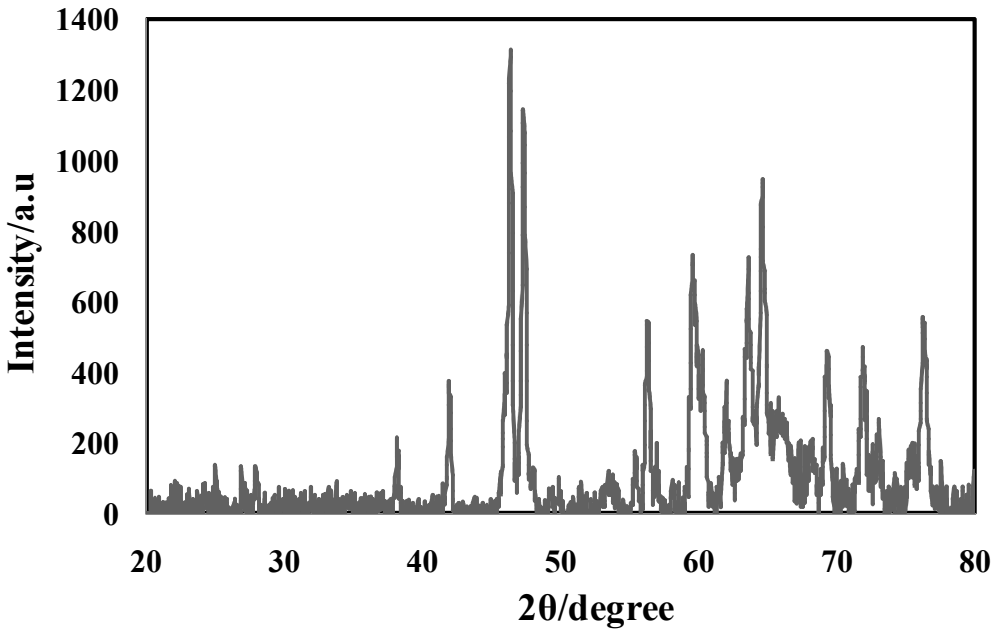

Figure 11: X-Ray diffraction pattern of proposed membrane sensor (E3) after used

Field Emission Scanning Electron Microscopy (FESEM) analysis on the membrane electrode was conducted to understand the morphological changes occurring during the electrode membrane preparation and after the destocking of fresh membrane into mercury(II) chloride solutions. The micrographs are presented in Figure 12. Scanning was done on the surface of electrode a, b and c at 50 μm range. A clear change in morphology of (a) HEMA-inner layer (b) after introducing a second layer proved that polypyrrole was successfully polymerized on the surface of electrode. The morphology also changes after the destocking of fresh membrane in mercury (II) chloride solutions with the appearance of the spherical shape of mercury atoms as can be seen in Figure 12(c). This can prove the complexation of mercury(II) with NHCL ionophores and its affinity towards the PPy membrane.

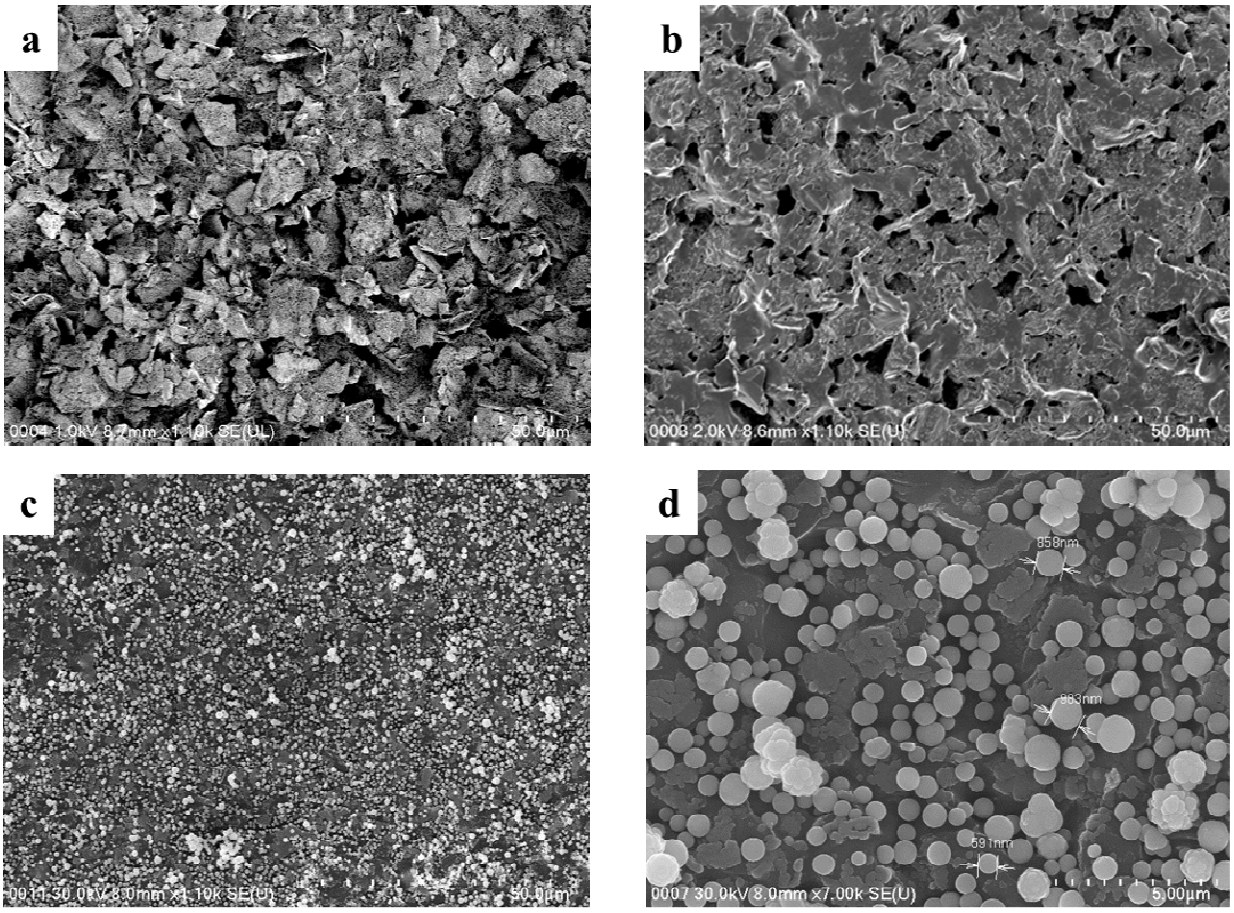

Figure 12: FESEM micrographs of membrane (E3): (**a**) HEMA-inner layer,(**b**) fresh optimized PPy membrane before and (**c**) after used and (**d**) enlargement from.

Energy Dispersive X-ray Analysis (EDX) was carried out on the surface of the used membrane. The EDX spectrum of optimized membrane is shown in Figure 13. It can be seen that there were only two elements, Hg and Br with traces of Cl found in the PPy membrane after use in the $HgCl_2$ solution (from 10^{-6} to 10^{-2}M). It further proves that the Hg^{2+} cations were successfully complexed to NHCL ionophore sites in the PPy matrix.

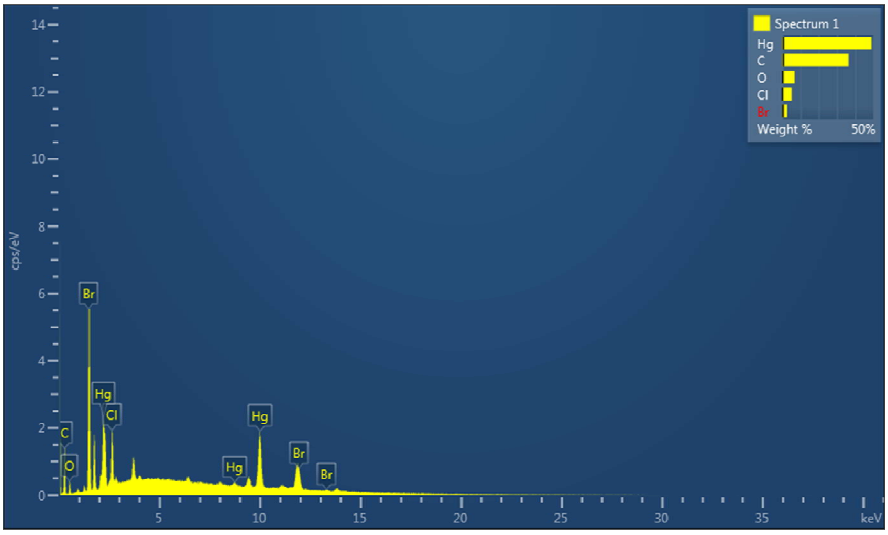

Figure 13 : EDX spectrum of optimized membrane (E3) after using in $HgCl_2$ solutions

3.8 Analytical application

The proposed Hg^{2+}-ISE was applied under laboratory conditions. It was successfully proved as an indicator electrode in the potentiometric titration of 25 ml Hg^{2+} solution (1.0×10^{-4} M) with EDTA (1.0×10^{-3} M). As shown in Figure 14, the obtained curve has an unsymmetrical shape. Moreover, the end point of the plot corresponds to 1:1 stoichiometry of EDTA-Hg^{2+} ions complex. The dash type in Figure 14 shows the plot of $\Delta E/\Delta V$ vs. mean volume of value of EDTA added. Before the end point, the potential demonstrated logarithmic changes with the volume of EDTA added, while it remained constant after the end point. The obtained potential decreased with the decrease in Hg^{2+} ion concentration due to their complexation with a standard EDTA solution. As a result, it is possible to determine the amount of Hg^{2+} ions in the solution accurately using the fabricated sensor.

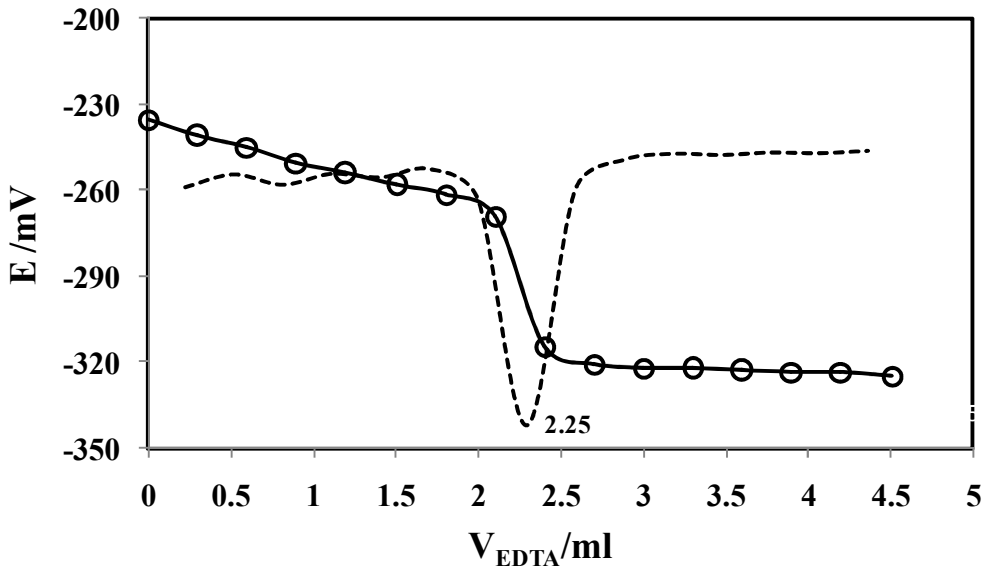

Figure 1: Application of proposed membrane sensor (E3) for the potentiometric titration of 25 ml 1.0×10^{-4} M Hg^{2+} solution with1.0×10^{-3} M EDTA.

In order to validate the accuracy of the proposed sensor based on NHCL ionophores in determining the concentration of Hg (II) cations, the determination of Hg (II) content in deionized water (DI water) and tap water samples were analyzed using the proposed sensor to detect Hg (II) concentrations via the spiked method (Table 9). The results approves that the amount of Hg(II) obtained by the proposed method agreed well with the added amount in the recovery range of % (104-140) demonstrating the acceptable performance of the supplied electrode for the recovery of mercury (II) content from water samples with difference matrices. Whereas, the relative standard deviation (RSD) values show readings which are lower than 5%, indicating the effectiveness of the proposed electrode. Moreover, the standard reference material (SRM) 2702 as a natural matrix of inorganic compounds was collected from marine sediment with certified concentration values and was used for proposed sensor validation [2, 48, 61]. As it can be seen, the results have good compatibility with certified ones (0.43 ppm). Therefore, the sensor can be a confidence device for determination of Hg(II) cation.

Table 9: Potentiometric determination of Hg^{2+}cation in DI water sample

	Hg^{2+} added, (M)	[a]Hg^{2+} Found, (M)	[b]Recovery, (%)	[c]RSD, (%)
DI Water	5.0×10^{-6}	5.7×10^{-6}	114.0	3.8
	5.0×10^{-5}	5.2×10^{-5}	104.0	4.3
	1.0×10^{-4}	1.4×10^{-4}	140.0	1.9
	5.0×10^{-3}	5.5×10^{-3}	110.0	1.7
Tap Water	5.0×10^{-6}	6.1×10^{-6}	122.0	2.8
	5.0×10^{-5}	5.9×10^{-5}	118.0	1.2
	1.0×10^{-4}	1.1×10^{-4}	110.0	4.1
SRM 2702	———	1.8×10^{-6}	———	0.6

[a]Average of three determination,
[b]Recovery= (found/added)×100,
[c]RSD= (SD/average)×100

3.9 Comparative study

The performance of proposed electrode is compared with the recently published mercury (II)-ISEs as shown in Table 10. Electrode numbers 1 to 8 were PVC-based membrane sensors for determining the mercury (II) cations. Meanwhile, electrode number 9 was a Hg^{2+}-selective electrode based on the self-plasticizing poly(n-butylacrylate) membrane sensor. With respect to those Hg(II)-ISE reported previously, the proposed electrode number 10 was compared. Summary data in Table 10 shows that, the proposed electrode gave better detection limits and response times compared to the previously suggested Hg^{2+}-self-plasticizing method. However, it exhibited a low detection limit in comparison to some Hg^{2+}-PVC membranes, yet still recording good response times in the detection of Hg^{2+} cations.

Table 10: Comparison of the proposed Hg^{2+} selective electrode with the previously reported electrode

No	Ionophore	Linear range (M)	Slope (mv decade^{-1})	Detection Limit (M)	Response Time (second)	Ref.
1	Ethyl-2-benzoyl-2-phenylcarbamoyl acetate (EBPCA)	1.0×10^{-6} -1.0×10^{-3}	30.0	7.0×10^{-7}	120	62
2	2-mercaptobenzothiazole (MBTH)	1.0×10^{-6} -1.0×10^{-1}	28.6	6.0×10^{-7}	20-100	63
3	4-(4-N,N-dimethylphenyl)-2,6-diphenylpyrilium tetrafluoroborate	1.0×10^{-8} -1.0×10^{-3}	34.0	1.0×10^{-8}	30-180	64
4	Calix[2]thieno[2]pyrrole	1.0×10^{-6} -1.0×10^{-1}	27.8	1.0×10^{-6}	20	65
5	Calixarene derivative	5.0×10^{-6} -1.0×10^{-2}	28.7	4.5×10^{-7}	20	59
6	Bis[5-((4-nitrophenyl)azo salicylaldehyde)] (BNAS)	7.0×10^{-7} -5.0×10^{-2}	30.0	2.0×10^{-7}	10	66
7	N,N-dimethylformamide-salicylacylhydrazone	6.2×10^{-7} -8.0×10^{-2}	29.6	5.0×10^{-7}	<30	67
8	Salicylaldehyde thiosemicarbazone	1.8×10^{-6} -1.0×10^{-1}	29.0	1.0×10^{-6}	<30	7
9	1,2-bis-(N'benzoylthioureido) cyclohexane	1.0×10^{-5}-1.0×10^{-1}	28.1	2.5×10^{-6}	50-100	34
10	7,10,13-triaza-1-thia-4,16-dioxa-6,14-dioxo-2,3;17,18-dinaphtho-cyclooctadecane (TDN)	1.0×10^{-8}-1.0×10^{-1}	29.6	7.0×10^{-9}	10	49
11	1,5-diphenylthiocarbazone (dithizone)	5×10^{-6} - 1×10^{-2}M	29.7	3.0×10^{-6}	15-30	50
12	4-(Dimethylamino)benzaldehyde 4-ethylthiosemicarbazone (DMABET)	5×10^{-6} - 1×10^{-1}M	27.8	5×10^{-6}	30	53
13	Kryptofix®5	1.0×10^{-8}-1.0×10^{-2}	42.0	1.0×10^{-7}	≤10	59

14	NHCL	1.0×10^{-6} -1.0×10^{-2}	28.16	2.5×10^{-7}	20	This work

3. Conclusion

This study revealed that the proposed Hg^{2+} selective electrode based on the synthesis of NHCL as ionophore can be used in the determination of Hg(II) cations in the concentration range of 1×10^{-6} to 1×10^{-2} M. It responded to the Hg^{2+} in a Nernstian slope of 28.10 ± 0.29 mV $decade^{-1}$ with good detection limits and response times at room temperature. This electrode can be classified as a new potentiometric self-plasticizing polypyrrole sensor which can solve the problem of PVC-based membrane sensors which requires plasticizers. The proposed membrane sensor was successfully used to determine various concentrations of mercury (II) in real samples with satisfactory results.

Acknowledgement

This research was supported by High Impact Research MoE Grant UM.C/625/1/HIR/MoE/SC/04 from Ministry of Education Malaysia, PPP Grant PG069-2012B and University Malaya Centre for Ionic Liquid (UMCiL). The author gratefully acknowledge to the UniversitiTeknologi Mara for a scholarship to pursue postgraduate studies.

References

1. M. E. Sears, K. J. Kerr and R. I. Bray, *J Environ Public Health*, 2012, 2012, 1-10.
2. S. B. T. Sany, A. Salleh, A. H. Sulaiman, A. Sasekumar, G. Tehrani and M. Rezayi, *Environment Protection Engineering*, 2012, 38, 139-155.
3. S. B. T. Sany, R. Hashim, A. Salleh, M. Rezayi and O. Safari, *Environmental Earth Sciences*, 2015, 1-11.
4. J. Wang, X. Feng, C. W. Anderson, Y. Xing and L. Shang, *Journal of Hazardous Materials*, 2012, 221-222, 1-18.
5. P. Holmes, K. James and L. Levy, *Science of The Total Environment*, 2009, 408, 171-182.
6. J. Mutter, J. Naumann, C. Sadaghiani, H. Walach and G. Drasch, *International Journal of Hygiene and Environmental Health*, 2004, 207, 391-397.
7. R. K. Mahajan, I. Kaur and T. S. Lobana, *Talanta*, 2003, 59, 101-105.
8. L. Y. Heng and E. A. Hall, *ASEAN Journal on Science and Technology for Development*, 2006, 23, 261-273.
9. L. Y. Heng and E. A. Hall, *Analytical chemistry*, 2000, 72, 42-51.
10. K. Mohammad, F. Aboufazeli, H. R. L. Zhad, O. Sadeghi and N. Ezzatollah, *Oriental journal of chemistry*, 2012, 28, 1557-1566.
11. M. Rezayi, Y. Lee, A. Kassim, S. Ahmadzadeh, Y. Abdollahi and H. Jahangirian, *Chem Cent J*, 2012, 6, 40.

12. M. Rezayi, R. Karazhian, Y. Abdollahi, L. Narimani, S. B. T. Sany, S. Ahmadzadeh and Y. Alias, *Scientific reports*, 2014, 4.
13. M. Rezayi, L. Y. Heng, A. Kassim, S. Ahmadzadeh, Y. Abdollahi and H. Jahangirian, *Sensors*, 2012, 12, 8806-8814.
14. A. Kassim, M. Rezayi, S. Ahmadzadeh, G. Rounaghi, M. Mohajeri, N. A. Yusof, T. W. Tee, L. Y. Heng and A. H. Abdullah, 2011.
15. F. Lorestani, Z. Shahnavaz, P. Mn, Y. Alias and N. S. Manan, *Sensors and Actuators B: Chemical*, 2015, 208, 389-398.
16. F. Lorestani, P. M. Nia, Y. Alias and N. S. Manan, *Journal of The Electrochemical Society*, 2015, 162, B193-B200.
17. M. Gholami, M. Rezayi, P. M. Nia, I. Yusoff and Y. Alias, *Measurement*, 2015, 69, 115-125.
18. M. Mahmoudian, Y. Alias, W. Basirun, P. MengWoi, F. Jamali-Sheini, M. Sookhakian and M. Silakhori, *Journal of Electroanalytical Chemistry*, 2015, 751, 30-36.
19. F. Lorestani, Z. Shahnavaz, P. M. Nia, Y. Alias and N. S. Manan, *Applied Surface Science*, 2015, 347, 816-823.
20. Y. Liu and J. Lynch, 2011.
21. P. Pawłowski, A. Michalska and K. Maksymiuk, *Electroanalysis*, 2006, 18, 1339-1346.
22. A. Michalska, *Electroanalysis*, 2005, 17, 400-407.
23. A. Kassim, M. Rezayi, S. Ahmad Zadeh, W. T. Tan, N. A. Yusof and Y. H. Lee, *Malaysian Journal of Chemistry*, 2009, 11, 19-25.
24. A. A. Abraham, M. Rezayi, N. S. Manan, L. Narimani, A. N. B. Rosli and Y. Alias, *Electrochimica Acta*, 2015, 165, 221-231.
25. M. Rezayi, M. Ghasemi, R. Karazhian, M. Sookhakian and Y. Alias, *Journal of The Electrochemical Society*, 2014, 161, B129-B136.
26. H. Mandil, A. Alhaj Sakur and B. Nasser, *International Journal of Pharmacy & Pharmaceutical Sciences*, 2013, 5, 423-428.
27. F. N. El-Dien, G. G. Mohamed, E. Y. Frag and M. E.-B. Mohamed, *Int. J. Electrochem. Sci*, 2012, 7, 10266-10281.
28. D. Nanda, M. Oak and M. P. Kumar, *Indian journal of chemistry. Section A, Inorganic, bio-inorganic, physical, theoretical & analytical chemistry*, 2007, 46, 258.
29. A. Radu, T. Radu, C. Mcgraw, P. Dillingham, S. Anastasova-Ivanova and D. Diamond, *Journal of the Serbian Chemical Society*, 2013, 78, 1729-1761.
30. S. Ahmadzadeh, M. Rezayi, H. Karimi-Maleh and Y. Alias, *Measurement*, 2015, 70, 214-224.
31. S. Ahmadzadeh, A. Kassim, M. Rezayi and G. H. Rounaghi, *Molecules*, 2011, 16, 8130-8142.
32. M. Rezayi, A. Kassim, S. Ahmadzadeh, A. Naji and H. Ahangar, *Int J Electrochem Sci*, 2011, 6, 4378-4387.
33. M. Rezayi, S. Ahmadzadeh, A. Kassim and Y. Lee, *Int J Electrochem Sc*, 2011, 6, 6350-6359.
34. J. Jumal, B. M. Yamin, M. Ahmad and L. Y. Heng, *APCBEE Procedia*, 2012, 3, 116-123.
35. H. Y. Jin, T. H. Kim, J. Kim, S. S. Lee and J. S. Kim, *Bulletin-korean chemical society*, 2004, 25, 59-62.

36. Y. Kitatsuji, H. Aoyagi, Z. Yoshida and S. Kihara, *Analytica chimica acta*, 1999, 387, 181-187.
37. R. A. Haque, A. W. Salman, T. S. Guan and H. H. Abdallah, *Journal of Organometallic Chemistry*, 2011, 696, 3507-3512.
38. M. V. Baker, D. H. Brown, R. A. Haque, B. W. Skelton and A. H. White, *Journal of Inclusion Phenomena and Macrocyclic Chemistry*, 2009, 65, 97-109.
39. Q.-X. Liu, H.-L. Li, X.-J. Zhao, S.-S. Ge, M.-C. Shi, G. Shen, Y. Zang and X.-G. Wang, *Inorganica Chimica Acta*, 2011, 376, 437-445.
40. W. A. Herrmann, *Angewandte Chemie*, 2002, 41, 1290-1309.
41. S. Díez-González and S. P. Nolan, *Coordination chemistry reviews*, 2007, 251, 874-883.
42. N. N. Al-Mohammed, Y. Alias, Z. Abdullah, R. M. Shakir, E. M. Taha and A. A. Hamid, *Molecules*, 2013, 18, 11978-11995.
43. B. M. Yamin, L. Narimani and N. Ibrahim, *International Journal on Advanced Science, Engineering and Information Technology*, 2013, 3, 47-49.
44. L. Narimani and B. M. Yamin, *Acta Crystallographica Section E: Structure Reports Online*, 2010, 66, 669-669.
45. L. Narimani and B. M. Yamin, *Acta Crystallographica Section E: Structure Reports Online*, 2012, 68, 1475-1475.
46. S. Budagumpi, R. A. Haque, A. W. Salman and M. Z. Ghdhayeb, *Inorganica Chimica Acta*, 2012, 392, 61-72.
47. Q.-X. Liu, L.-X. Zhao, X.-J. Zhao, Z.-X. Zhao, Z.-Q. Wang, A.-H. Chen and X.-G. Wang, *Journal of Organometallic Chemistry*, 2013, 731, 35-48.
48. S. B. T. Sany, A. Salleh, M. Rezayi, N. Saadati, L. Narimany and G. M. Tehrani, *Water, Air, & Soil Pollution*, 2013, 224, 1-18.
49. F. Tadayon, A. Katebi, A. Afkhami, Y. Panahi and H. Bagheri, *International Journal of Environmental Analytical Chemistry*, 2014, 94, 901-915.
50. A. K. Hassan, *Modern Chemistry & Applications*, 2013, 1, 1-4.
51. N. Zhou, H. Chen, J. Li and L. Chen, *Microchimica Acta*, 2013, 180, 493-499.
52. M. Ganjali, F. Faridbod, N. Davarkhah, S. Shahtaheri and P. Norouzi, *Int. J. Environ. Res*, 2015, 9, 333-340.
53. T. F. Tahir, A. Salhin and S. A. Ghani, *Sensors*, 2012, 12, 14968-14982.
54. R. P. Buck and E. Lindner, *Pure and Applied Chemistry*, 1994, 66, 2527-2536.
55. P. M. Nia, W. P. Meng, F. Lorestani, M. Mahmoudian and Y. Alias, *Sensors and Actuators B: Chemical*, 2015, 209, 100-108.
56. P. M. Nia, F. Lorestani, W. P. Meng and Y. Alias, *Applied Surface Science*, 2015, 332, 648-656.
57. M. H. Mashhadizadeh, S. Ramezani and M. K. Rofouei, *Materials Science and Engineering: C*, 2015, 47, 273-280.
58. R. Mahajan, I. Kaur, V. Sharma and M. Kumar, *Sensors*, 2002, 2, 417-423.
59. A. A. Ismaiel, M. K. Aroua and R. Yusoff, *American Journal of Analytical Chemistry*, 2012, 3, 859-865.
60. Y. Umezawa, P. Bühlmann, K. Umezawa, K. Tohda and S. Amemiya, *Pure and Applied Chemistry*, 2000, 72, 1851-2082.
61. S. B. T. Sany, A. Salleh, A. H. Sulaiman, A. Sasekumar, M. Rezayi and G. M. Tehrani, *Environmental earth sciences*, 2013, 69, 2013-2025.

62. S. S. Hassan, M. B. Saleh, A. A. A. Gaber, R. A. Mekheimer and N. A. A. Kream, *Talanta*, 2000, 53, 285-293.
63. M. Mazloum, M. K. Amini and I. Mohammadpoor-Baltork, *Sensors and Actuators B: Chemical*, 2000, 63, 80-85.
64. X. Yu, Z. Zhou, Y. Wang, Y. Liu, Q. Xie and D. Xiao, *Sensors and Actuators B: Chemical*, 2007, 123, 352-358.
65. I. I. Abbas, *International Journal of Chemistry*, 2012, 4, 23-29.
66. M. H. Mashhadizadeh and I. Sheikhshoaie, *Talanta*, 2003, 60, 73-80.
67. G. Ye, Y. Chai, R. Yuan and J. DAI, *Analytical sciences*, 2006, 22, 579-582.